

Stochastic Sensitivity in Homogeneous Electromagnetic-Thermal Dosimetry Model of Human Brain

Mario Cvetković¹, Sébastien Lalléchère², Khalil El Khamlichi Drissi², Pierre Bonnet², and Dragan Poljak¹

¹FESB, University of Split, Split, Croatia
(mcvetkov, dpoljak)@fesb.hr

²Institut Pascal, Université Blaise Pascal, Clermont-Ferrand, France
(sebastien.lallechere, drissi, pierre.bonnet)@lasmea.univ-bpclermont.fr

Abstract— In this work we examined how the variability in the brain morphology and the tissue properties affect the assessment of the homogeneous human brain exposed to high frequency electromagnetic (EM) field. Using the deterministic EM-thermal modeling and the stochastic theoretical basis we have studied the effects of these uncertainties on the maximum induced electric field, maximum local Specific Absorption Rate (SAR), average SAR, maximum temperature and the maximum temperature increase, respectively. The results show a good convergence of stochastic technique and an assessment of mean and variance of outputs for the incident plane wave of 900 MHz.

Index Terms— Bioelectromagnetism, electromagnetic-thermal model, sensitivity analysis, statistical dosimetry, stochastic collocation, surface integral equation approach.

I. INTRODUCTION

The exposure of a modern man to electromagnetic (EM) fields has raised some questions regarding the potentially harmful effects on the human health. This is, in particular, the case for the human head and brain exposed to high frequency (HF) radiation. The HF exposure assessment is based on the calculation of SAR distribution and the related temperature rise. As measurement of induced fields is not possible, human exposure assessment is carried out by using appropriate computational models. One difficulty of the modeling lies in the fact that values of the various model parameters can vary considerably due to, e.g., possible difference in individual size, but also due to different age (morphology) [1], or the general variability of electrical parameters such as permittivity and electrical conductivity [2], again, due to difference in age or sex. This uncertainty of the input parameters can result in the uncertainty of the dosimetric model outputs such as

induced electric field and SAR. Thus, one of the key challenges that numerical dosimetry faces today is management of these uncertainties [3]. A novel approach to this problem, that is attracting more and more attention [4]-[7] is the so called stochastic dosimetry, combining deterministic electromagnetic techniques with the statistical methods.

The uncertainties that are discussed in this paper cover only a small subset of a huge variability apparent in the dosimetry literature due to variations in the exposure parameters and the anatomic variability of people [8], [9]. Review in [8] classified these differences due to the age dependent tissue dielectric properties, anatomically based models from children and adults of varying age and race, effects of pinna on SAR, distributions of SAR within the brain, and the effects of variability among models on SAR, respectively.

This paper presents the deterministic electromagnetic-thermal model coupled with the stochastic theoretical basis. The model is used to examine the effects of the variability in the brain morphology and the tissue properties on the dosimetric assessment in case of homogeneous human brain exposed to high frequency EM field. The sensitivity analysis of various parameters in this simplified model could thus aid in better formulation of a more realistic and computationally much more demanding models.

The paper is organized as follows. In the first part, description of the electromagnetic-thermal model proposed to compute SAR and temperature outputs is given. The following part gives details about the stochastic technique used jointly with previous model to propagate uncertainties. Finally, the numerical results for the case of brain exposed to radiation of vertically and horizontally polarized 900 MHz plane wave, respectively, are given with the corresponding statistical outputs.

II. DETERMINISTIC MODEL

A. Electromagnetic dosimetry model

The electromagnetic model is based on the surface integral equation (SIE) formulation [10], and, methodologically, represents a fresh perspective in the bioelectromagnetics area dominated mostly by the differential equation based methods such as FDTD (finite difference time domain). In addition to high accuracy, the advantages of the SIE formulation include: discretization of only boundary of the problem, hence reducing the dimensionality of the problem, it is suitable for open boundary problems (such as human head exposed to EM field), it gives exact solution to open boundary problem (no need to artificially limit the domain), does not suffer from staircasing errors related to FDTD, etc. Regardless of all these advantages, the integral equation approach has only recently begun its revival in the bioelectromagnetics community [11], [12].

It must be noted that the SIE formulation is only one way of transforming the original boundary value problem of Maxwell's equations into an integral equation form. The same problem could also be formulated using the volume integral equation (VIE), but then one loses the dimensionality reduction, in addition to having to deal with tensor-type integral equation and dyadic Green's functions. The choice of the particular integral technique will be primarily dependent on the domain problem type. Interested reader could find more details in [13], [14].

To set up the EM model, the human brain is considered as a lossy homogeneous dielectric material with complex permittivity and permeability (ϵ, μ) , placed in a free space. The complex permittivity of the brain is given by:

$$\epsilon = \epsilon_0 \epsilon_r - j \frac{\sigma}{\omega}, \quad (1)$$

while the value for the permeability of the brain is taken to be μ_0 , i.e., the free space permeability, due to the fact that biological tissues do not possess magnetic properties. It is important to mention that human tissues have chiral characteristics, the property intrinsic to many biological molecules as well as human cells [15], meaning that the magnetic field will affect the electric flux and the electric field will affect the magnetic flux through material properties. But to the best of authors knowledge, there are no relevant study on this property for the human brain, hence, it was not taken into account.

The brain is exposed to a radiation of plane 900 MHz EM wave of power density of $P=5$ mW/cm². Using the equivalence theorem, two equivalent problems are formulated in terms of the equivalent electric and magnetic current densities placed on the surface of the brain. After the application of boundary condition at the surface S being interface of the two equivalent problems, the coupled set of integral equations is obtained:

$$j\omega\mu_i \int_S \vec{J}(\vec{r}') G_i dS' - \frac{j}{\omega\epsilon_i} \nabla \int_S \nabla' \cdot \vec{J}(\vec{r}') G_i dS' + \nabla \times \int_S \vec{M}(\vec{r}') G_i dS' = \begin{cases} \hat{n} \times \vec{E}^{inc}; & i = 1 \\ 0 & ; i = 2 \end{cases} \quad (2)$$

where \vec{E}^{inc} is the known incident field, \vec{J} and \vec{M} represent the unknown surface currents, while i is index of medium. The equivalent electric and magnetic currents \vec{J} and \vec{M} are expressed by the linear combination of RWG and $\hat{n} \times \text{RWG}$ basis functions, respectively, defined on a pair of triangles.

The numerical solution of Eq. (2) is done via an efficient scheme of a method of moments (MoM) leading to a matrix type equation whose solution is a vector containing the unknown coefficients J_n and M_n . From these coefficients, the equivalent currents \vec{J} and \vec{M} can be determined from:

$$\vec{J}(\vec{r}) = \sum_{n=1}^N J_n \vec{f}_n(\vec{r}), \quad (3)$$

$$\vec{M}(\vec{r}) = \sum_{n=1}^N M_n \vec{g}_n(\vec{r}), \quad (4)$$

where \vec{f}_n and \vec{g}_n are known basis functions.

Subsequently, the electric field can be determined at an arbitrary point in brain using the following:

$$\vec{E}(\vec{r}) = -j\omega\mu \int_S \vec{J}(\vec{r}') G(\vec{r}, \vec{r}') dS' - \frac{j}{\omega\epsilon} \int_S \nabla' \cdot \vec{J}(\vec{r}') G(\vec{r}, \vec{r}') dS' - \int_S \vec{M}(\vec{r}') \times \nabla G(\vec{r}, \vec{r}') dS'. \quad (5)$$

From the electric field distribution inside the brain, the specific absorption rate (SAR) is readily found using:

$$SAR = \frac{\sigma}{2\rho} |\vec{E}|^2, \quad (6)$$

where ρ is the brain tissue density given in kg/m³. SAR is latter used as input to the thermal part of the model.

B. Thermal dosimetry model

The experimental measurements of brain thermal response due to EM radiation is not possible in healthy humans. As indirect methods such as magnetic resonance imaging (MRI) lack sufficient resolution, and using animals as surrogate models raises the question of interspecies difference, the computational modeling seems to be the only alternative. It should be noted that the bioheat equation used for the kind of application presented here, has not been validated experimentally, and hence, presents forward only model.

The problem of determining the temperature distribution in the human brain is addressed using the finite element method (FEM). The steady-state temperature distribution in the brain, exposed to an incident time harmonic electromagnetic (EM) field, is governed by the stationary form of the Pennes' bioheat Equation [16]:

$$\nabla \cdot (\lambda \nabla T) + W_b c_b (T_a - T) + Q_m + Q_{ext} = 0, \quad (7)$$

where the heat generated due to metabolic processes is given by Q_m , W_b and c_b are the volumetric perfusion rate and the specific heat capacity of blood, respectively, λ is the thermal conductivity of the tissue, and T_a is the arterial

blood temperature. The last term in (7) represents the amount of heat generated due to absorption of EM energy in the tissue, and can be calculated from:

$$\mathbf{Q}_{ext} = \rho \cdot \mathbf{SAR}. \quad (8)$$

The equation (7) is supplemented by the Robin boundary condition, while the heat loss due to radiation, and the forced convection are neglected. The finite element formulation of (7) is based on the weighted residual approach. The approximate solution of (7) is expanded in terms of the known basis functions and the unknown coefficients. After multiplying (7) by a set of weighting functions and integrating over the domain, after some work, we arrive to a suitable expression for the finite element method implementation:

$$\begin{aligned} & \iiint_{\Omega} \lambda \nabla T \cdot \nabla N_j d\Omega + \iiint_{\Omega} \mathbf{W}_b T N_j d\Omega + \\ & \iint_{\partial\Omega} \mathbf{h}_s T N_j dS = \iiint_{\Omega} (\mathbf{W}_b T_a + \mathbf{Q}_m + \mathbf{Q}_{ext}) N_j d\Omega + \\ & \iint_{\partial\Omega} \mathbf{h}_s T_{amb} N_j dS. \end{aligned} \quad (9)$$

The processing part of the electromagnetic and the thermal dosimetry models was carried out using authors developed code.

C. The homogeneous human brain

Although the presented formulation could be used on a more detailed brain surface model built from an MRI, the source of the brain model was a freely available template from a Google Sketchup library. Assuming the dimensions of the average adult human brain are: width 131.8 mm, length 161.1 mm, height 139 mm, the frequency dependent parameters of the human brain are taken from [17]. The value for the relative permittivity and the electrical conductivity of the brain are given by $\epsilon_r=45.805$ and $\sigma=0.766$ S/m, respectively, taken as the average values between white and gray matter at 900 MHz. Assuming each of the previous parameter may be impacted by random variations uniformly distributed, the following part will be dedicated to the propagation of uncertainties and discussion about numerical results.

III. STOCHASTIC MODELING

Complementary to solid deterministic modeling, stochastic techniques [1], [18] are helpful to precisely assess statistics of a given mapping and provide its sensitivity analysis.

A. Propagation of uncertainties

First, five random variables (RVs) are solely considered and devoted to the representation of parameters assumed as uncertain ones: brain's width (RV₁), length (RV₂), height (RV₃), relative dielectric permittivity ϵ_r (RV₄) and conductivity σ (RV₅). At this stage, and for the sake of simplicity, the RVs are loosely assumed to be independent and identically distributed (iid) following Uniform laws. Even though this point may be criticized, particularly related to morphing of

geometrical parameters, we may consider this as the first-order assumption. Indeed, there are solutions that easily integrate dependencies in stochastic collocation (SC) methods and the following methodology will still be valuable with iid-RVs. Assuming each RV_k (k=1,...,5) is uniformly distributed around values from part II-C with common coefficient of variation (CV) equal to 5.77% [19], this first approach may offer a rapid estimation of potential importance of RVs. On the other hand, the study of a complete RV set is necessary, taking into account their interdependence, as is the case for morphological parameters [1].

B. Stochastic collocation theoretical basis

Among the different stochastic techniques available in the literature, the non-intrusive stochastic collocation (SC) method [18] was used in this dosimetric framework. The method is part of spectral approaches [20]. Similarly to strategies developed for Monte Carlo (MC) methods [21], the aim of these sampling techniques is to lead efficient experimental design (e.g., by decreasing the number of input samples needed). The basis of spectral techniques relies on a polynomial expansion of the considered output (e.g., u -th statistical moment of electric field, $[E]^u$) for given random parameters (Z_1, Z_2, \dots, Z_N) where each Z_k ($k = 1, \dots, N$) is defined from one given RV RV_k as:

$$Z_k = Z_k^0 + RV_k, \quad (10)$$

where Z_k^0 is the initial (mean) value and RV_k is RV with assigned statistical distribution.

By assuming random parameter Z_k , the random output of interest E ($E \equiv [E]^u$) is expanded over the stochastic space using the Lagrangian bases set [18]:

$$E(Z_k^0; t) = \sum_{i=0}^n E_i(Z_k^0) L_i(t), \quad (11)$$

where $L_i(t)$ is Lagrange polynomial given by:

$$L_i(t) = \prod_{j=1, j \neq i}^n \frac{(t-t_j)}{(t_j-t_i)}. \quad (12)$$

Utilizing the property of Lagrangian basis, yields:

$$E_i(Z_k^0) = E(Z_k^0; t_i). \quad (13)$$

Applying the rules for the assessment of statistical moments on equation (10), the mean and the variance are easily derived, respectively:

$$[E(Z_k^0; t)]^1 = \sum_{i=0}^n \omega_i E_i(Z_k^0), \quad (14)$$

$$[E(Z_k^0; t)]^2 = \sum_{i=0}^n \omega_i \{E_i(Z_k^0) - [E(Z_k^0; t)]^1\}^2, \quad (15)$$

where ω_i is given by integral:

$$\omega_i = \int_D L_i(t) p(t) dt, \quad (16)$$

where $p(t)$ denotes the probability density function of RV_k .

The order of approximation of the output E , i.e., the convergence, depends on number of collocation points t_i . The computation of integral (16) is carried out using Gaussian quadrature.

In a more general case, when extending the relations (14) and (15) to multi-RVs (e.g., case with N RVs), Lagrangian basis is used to approximate mapping $[E]^u$

as follows:

$$[E]^u(\mathbf{R}) = \sum_{v_1=0}^{n_1} \dots \sum_{v_N=0}^{n_N} \eta_{v_1 \dots v_N}^u \Phi^u(\mathbf{R}), \quad (17)$$

where $\mathbf{R} = (RV_1, RV_2, \dots, RV_N)^T$ is called random vector (i.e., vector containing the N random parameters of the problem), $\Phi^u(\mathbf{R})$ is related to the chosen polynomial expansion, and $\eta_{v_1 \dots v_N}^u$ are the weights dedicated to SC points, respectively. Relation (17) implies $n_w + 1$ ($w = 1, \dots, N$) SC points (SC n_w order expansion) to compute random component R_w in a straightforward manner.

For the interested reader, the developments and choice of Lagrangian polynomial basis are explained in [18], [22]. It is to be noticed that previous approach is proposed assuming the independence of random parameters. Similarly to alternative Unscented Transform (UT) sampling technique [23], taking into account correlation of RVs is possible throughout covariance matrix, and finally transform initial sigma points, keeping the same strategy as previously exposed. Computing statistical moments will be straightforward as depicted in relation (17).

C. Numerical results from 1-RV mean contributions

Using our deterministic EM model, the distribution of the electric field in our human brain model is determined, as shown in Fig. 1.

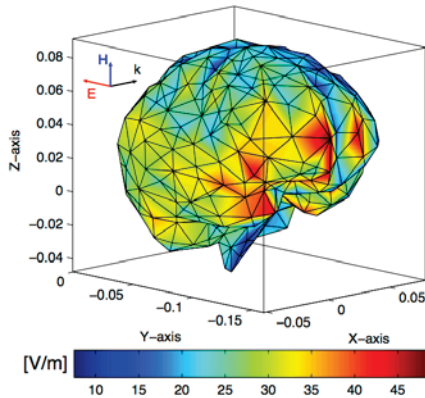


Fig. 1. Distribution of electric field on the brain surface. Horizontally polarized plane wave of frequency 900 MHz, power density $P=5 \text{ mW/cm}^2$.

From the distribution of the electric field inside the brain, the SAR is determined next. The resulting SAR will cause a certain temperature increase, ΔT , determined using our thermal dosimetry model. As the incident wave's polarization presents an important role in the assessment of the electric field and the related SAR, all calculations were carried out for two polarizations of the incident plane wave: vertical and horizontal. Figures 2 and 3 show the results for the temperature rise in the human brain, due to horizontally and vertically polarized wave, respectively.

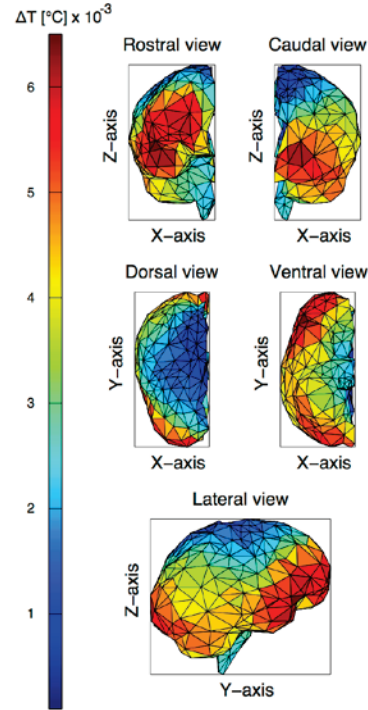


Fig. 2. Temperature rise in the human brain model due to incident 900 MHz horizontally polarized plane wave, power density $P=5 \text{ mW/cm}^2$.

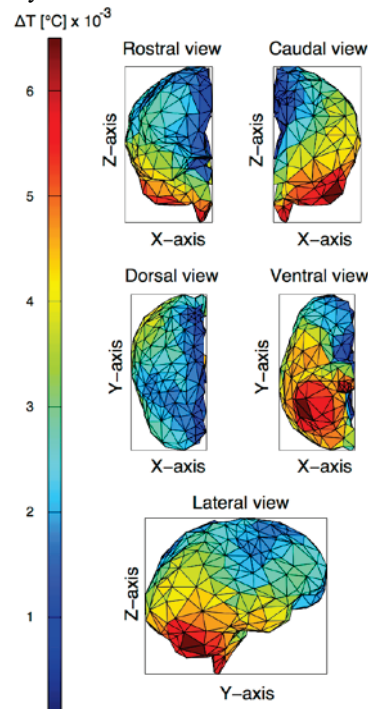


Fig. 3. Temperature rise in the human brain model due to incident 900 MHz vertically polarized plane wave, power density $P=5 \text{ mW/cm}^2$.

Figure 4 shows the SC convergence of maximum electric field mean value for different RVs ($RV_k; k = 1, \dots, 5$) by taking into account the increasing number of points in SC experimental design (e.g., 3, 5, 7 points). Although the output (maximum SAR) is highly non linear, SC offers a precise assessment of its first statistical moment with 5 multi-physics simulations. It can be observed that the mean of the maximum E-field is between 48.8 and 49.8 V/m, indicating the importance of modeling RVs at the same time.

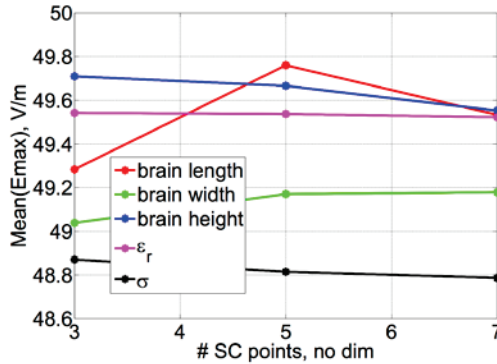


Fig. 4. Mean of maximum electric field in function of number of SC points (3, 5, 7) at frequency 900 MHz.

On the other hand, Fig. 5 shows the potential influence the individual random variables have on the variance of the maximum E-field. Similar to the case of mean assessment, the SC technique provides trustworthy results even with only 3 simulations.

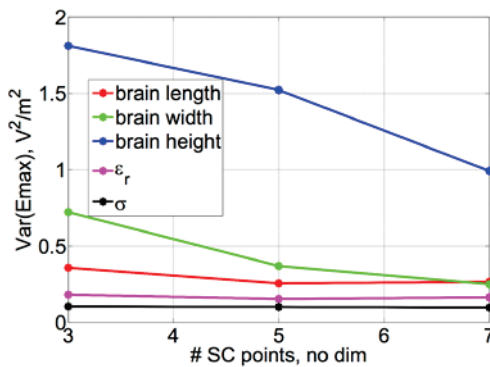


Fig. 5. Variance of maximum electric field in function of number of SC points (3, 5, 7) at frequency 900 MHz.

Similar to Figs. 4 and 5, the SC efficiency and convergence is assessed in Figs. 6 and 7 where mean and variance of a non-linear thermal parameter (temperature rise in brain) is given. A trustworthy result is obtained regarding independently each RV with only 3 full-wave

simulations.

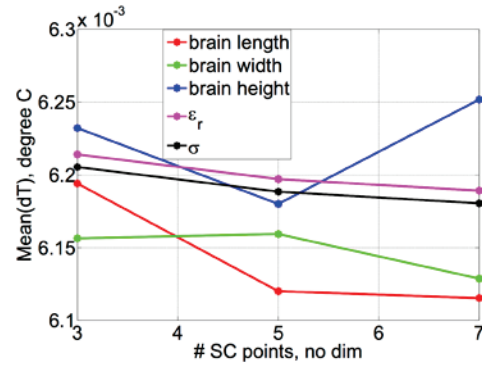


Fig. 6. Mean of temperature rise in function of number of SC points (3, 5, 7) at frequency 900 MHz.

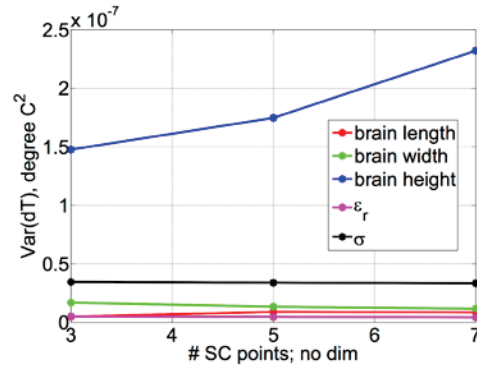


Fig. 7. Variance of temperature rise in function of number of SC points (3, 5, 7) at frequency 900 MHz.

In order to complement the preliminary results obtained with only 1-RV modeling, Tables 1 and 2 give an overview of the statistics obtained from a stochastic model including all RVs for both polarizations. Mean and variances obtained for each of the given outputs (maximum E-field, maximum SAR, averaged SAR, maximum temperature, temperature rise), considering a whole model including 5 RVs are presented. As expected, there are differences between the entire stochastic approach and 1-RV modeling. The experimental design chosen in this example is based upon 243 simulations (approaching each statistical moments using only 3 SC points for each RV, leading to $3^5=243$ simulations). Of course, some alternative approaches are practicable but the crude tensor product (i.e. full-tensorized SC) given by relation (17) offers confidence related to the accuracy of the computed data. It should be noticed that the convergence of results has been checked (data not shown here) by using full-tensorized model with 5 SC points for each RV.

Table 1: SC results (mean/variance, var.) for given outputs (one may notice units are given for means; 1: maximum electric field in V/m, 2: maximum SAR in W/kg, 3: mean SAR in W/kg, 4: temperature in Celsius degrees, 5: temperature rise in Celsius degrees) for vertical (VV) polarization

Output	1	2	3	4	5
Output	49.9	0.9	0.16	37.1	6.1E-3
Var.($\times 10^4$)	37756	61.5	0.7	1.3	2.0E-3

Table 2: SC results (mean/variance, var.) for given outputs (one may notice units are given for means; 1: maximum electric field in V/m, 2: maximum SAR in W/kg, 3: mean SAR in W/kg, 4: temperature in Celsius degrees, 5: temperature rise in Celsius degrees) for horizontal (HH) polarization

Output	1	2	3	4	5
Output	48.7	0.9	0.17	37.0	7.3E-3
Var.($\times 10^4$)	23205	21.3	0.7	1.2	1.9E-3

D. Sensitivity analysis

A large diversity of techniques are available in [24] to assess the sensitivity analysis of various models. In the following, variance-based criteria are defined from SC data to assess the sensitivity of each random parameter (similarly to Sobol's first indices [24] but restricted to a qualitative evaluation). Indeed, for each given physical output j (where $j = 1, \dots, 5$ stands respectively for maximum E-field, maximum SAR, mean SAR, maximum temperature, and temperature rise):

$$I_i^j = \frac{V_i^j}{V^j}, \quad (18)$$

with i the RV indice (i.e., $i = 1, \dots, 5$), V_i^j variance relative to RV i and output j , V^j represents variance of output j computed from 5-RVs stochastic model, and I_i^j is the aforementioned influence criterion. It should be noticed here that, assuming extension to dependent random variables (see Section III), the relation (18) is still valuable to assess RV "global" sensitivity.

Figures 8 and 9 show the influence of the different random parameters relative to the variance obtained from the entire (e.g., 5-RVs) stochastic model following relation (18), for both polarizations. Close to global sensitivity analysis [24], this offers a qualitative overview of the impact of different RVs over various outputs. As expected, the results are highly problem-dependent, implying the choice of the output may influence the SC experimental design needed for a complete stochastic modeling of the problem. In this

framework, Tables 3 and 4 provide a ranking of the most influential parameters depending on the output, for vertical and horizontal polarization, respectively.

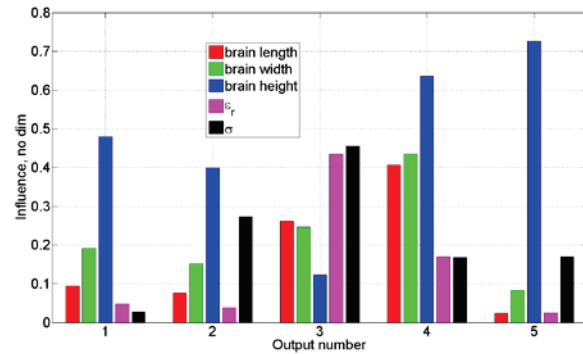


Fig. 8. Influence criterion I_i^j in function of outputs (1: E-field, 2: maximum SAR, 3: mean SAR, 4: max temperature, 5: temperature rise) and RV (brain's length, brain's width, brain's height, relative permittivity (ϵ_r) brain, conductivity (σ) brain) for vertical polarization.

Table 3: RV ranking from most (A) to least (E) influential parameters and given outputs (in relation with results in Fig. 8)

Output	1	2	3	4	5	Total
RV1: brain's length	C	D	C	C	E	D
RV2: brain's width	B	C	D	B	C	B
RV3: brain's height	A	A	E	A	A	A
RV4: ϵ_r brain	D	E	B	D	D	E
RV5: σ brain	E	B	A	E	B	C

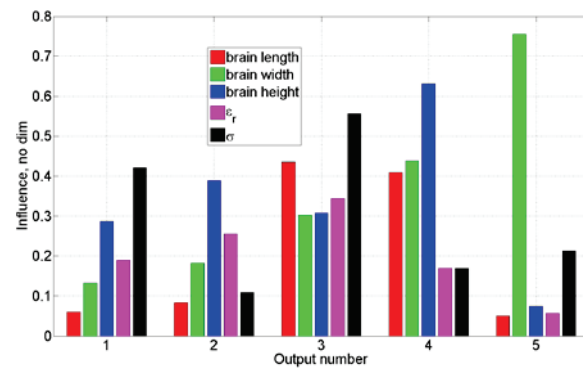


Fig. 9. Influence criterion I_i^j in function of outputs (1: E-field, 2: maximum SAR, 3: mean SAR, 4: max temperature, 5: temperature rise) and RV (brain's length, brain's width, brain's height, relative permittivity (ϵ_r) brain, conductivity (σ) brain) for horizontal polarization.

Table 4: RV ranking from most (A) to least (E) influential parameters and given outputs (in relation with results in Figure 9)

Output	1	2	3	4	5	Total
RV1: brain's length	E	E	B	C	E	E
RV2: brain's width	D	C	E	B	A	C
RV3: brain's height	B	A	D	A	C	A
RV4: ϵ_r brain	C	B	C	D	D	D
RV5: σ brain	A	D	A	E	B	B

E. Discussion

Due to the multi-physics of the problem (thermal and electromagnetic), the sensitivity of the statistical model is different from a given output to another.

As expected, conductivity σ seems to play a key role for SAR assessment (especially regarding mean value) (Tables 3 and 4). Contrary to σ , relative permittivity seems to produce weaker effects both considering EM and thermal outputs. Regarding geometrical parameters, brain's height seems to play a major role both considering thermal outputs and maximum electric ones (out of averaged SAR); this might be expected due to chosen EM sources (plane wave's orientation); brain's length and width are less influential in that case.

Similarly to thermal differences due to horizontal (Fig. 2) and vertical (Fig. 3) polarizations, EM sources involve various results when considering influence of each random parameter. Vertical polarization strengthens the importance of geometrical brain's parameters comparatively to geometrical ones except for averaged SAR since ϵ_r and σ are key parameters. The relative influence of materials is high for horizontal polarized wave regarding EM outputs. This validates the interest of the proposed methodology as a framework for sensitivity analysis combining deterministic and stochastic models.

From past discussions, an adaptation of the experimental design is possible. Thus, the least influential variables may be considered with a restricted number of points (e.g., changing some parameters to deterministic ones or withdrawing some inputs in the initial experimental design [25]), whereas the most effort may be put on the most influential ones.

Although the focus of presented paper was on the proposed methodology as a framework for sensitivity analysis combining deterministic and stochastic models, some limitations regarding the deterministic model should be addressed at this point. The homogeneous brain model insulated in free space does not represent a realistic scenario. As the actual brain is surrounded by various other tissues, such as e.g. cerebrospinal fluid, fat, skull and scalp, the overall electric field distribution and the related SAR will be affected due to these tissues. The work related to the inclusion of the surrounding tissues such as skull and scalp is currently under way. In order

to take into account this type of scenario, it will be necessary to use a different integral equation formulation, such as a tensor-type volume integral equation approach.

Furthermore, the low number of triangular elements used to represent the surface of our model results in the less smooth appearance of the electric field. The brain surface model presented in this paper is smoothed out neglecting the detailed cortical structures, although the proposed integral equation formulation is applicable to an arbitrarily shaped biological tissue, including a more detailed brain model taking into account the cortex foldings. The downside of the detailed description of the brain is the total number of elements required to accurately represent the geometry. This would consequently lead to a very large matrix system whose solution would require the use of advanced techniques such as multilevel fast multipole algorithm and hence prevents our model at present stage in doing so.

Finally, the presented framework did not take into account the variability of thermal parameters such as the heat generated due to metabolic processes Q_m , the volumetric perfusion rate and the specific heat capacity of blood, W_b and c_b , respectively, the thermal conductivity of the tissue λ , and the arterial blood temperature T_a . The influence of these thermophysiological parameters on the induced SAR and the related temperature distribution related to the thermal dosimetry model is required due to their variability as well as general uncertainty [26], [27].

IV. CONCLUSION

One of the challenges the electromagnetic-thermal dosimetry models face is related to the uncertainty of the various input parameters. To overcome this, the stochastic dosimetry approach will be necessary, where both stochastic and deterministic models are used. Based upon a deterministic model coupling EM and thermal dosimetry, this contribution proposes to integrate uncertain variations around input parameters. The expansion of statistical outputs (e.g., mean and variance) over a polynomial basis (via SC) showed robustness and efficiency (limited size of experimental design) both for EM and temperature quantities.

The quantitative computing of statistical first and second order moments enables a qualitative sensitivity study in order to focus on the most influential parameters. From this analysis, a competitive and efficient model may be defined for instance in order to perform a more demanding computing (e.g., in order to provide probability density function, assess reliability analysis, and put the focus on extreme values). From an optimized statistical model, we may also achieve richer EM and thermal description of the brain's behavior by increasing the number of random variables and their complexity.

ACKNOWLEDGMENT

The author M. Cvetković would like to thank I. Tomac from the Department of Mechanical Engineering and Naval Architecture, and M. Despalatović and Ž. Gladina from the Department of Electrical Engineering, University of Split, for the computational resources provided.

REFERENCES

- [1] A. E. Habachi, et al., "Statistical analysis of whole-body absorption depending on anatomical human characteristics at a frequency of 2.1 GHz," *Phys. Med. Biol.*, vol. 55, no. 7, pp. 1875-1887, 2010.
- [2] R. L. McIntosh and V. Anderson, "A comprehensive tissue properties database provided for the thermal assessment of a human at rest," *Biophysical Reviews and Letters*, vol. 5, no. 3, pp. 129-151, 2010.
- [3] J. Wiart, et al., "Handle variability in numerical exposure assessment: The challenge of the stochastic dosimetry," in *Antennas and Propagation (EuCAP), 2013 7th European Conference on*, pp. 1979-1981, 2013.
- [4] O. Aiouaz, et al., "Uncertainty analysis of the specific absorption rate induced in a phantom using a stochastic spectral collocation method," *Annals of Telecommunications*, vol. 66, no. 7-8, pp. 409-418, 2011.
- [5] I. Liorni, et al., "Polynomial chaos decomposition applied to stochastic dosimetry: Study of the influence of the magnetic field orientation on the pregnant woman exposure at 50 Hz," in *Engineering in Medicine and Biology Society (EMBC), 2014 36th Annual International Conference of the IEEE*, pp. 342-344, 2014.
- [6] D. Voyer, et al., "Probabilistic methods applied to 2D electromagnetic numerical dosimetry," *COMPEL*, vol. 27, no. 3, pp. 651-667, 2008.
- [7] P. Kersaudy, et al., "A new surrogate modeling technique combining kriging and polynomial chaos expansions - application to uncertainty analysis in computational dosimetry," *J. Comput. Phys.*, vol. 286, no. 1, pp. 103-117, 2015.
- [8] K. R. Foster and C.-K. Chou, "Are children more exposed to radio frequency energy from mobile phones than adults?," *Access, IEEE*, vol. 2, pp. 1497-1509, 2014.
- [9] J. Wiart, et al., "Analysis of RF exposure in the head tissues of children and adults," *Phys. Med. Biol.*, vol. 53, no. 13, pp. 3681-3695, 2008.
- [10] M. Cvetković and D. Poljak, "An efficient integral equation based dosimetry model of the human brain," in *Proceedings of 2014 International Symposium on Electromagnetic Compatibility (EMC EUROPE) 2014*, Gothenburg, Sweden, pp. 375-380, 1-4 September 2014.
- [11] F. Wei and A. Yilmaz, "A more scalable and efficient parallelization of the adaptive integral method—part ii: Bioem application," *IEEE T. Antenn. Propag.*, vol. 62, no. 2, pp. 727-738, 2014.
- [12] M. Cvetkovic, D. Poljak, and J. Haueisen, "Analysis of transcranial magnetic stimulation based on the surface integral equation formulation," *IEEE T. Bio-Med. Eng.*, vol. 62, no. 6, pp. 1535-1545, 2015.
- [13] W. C. Chew, M. S. Tong, and B. Hu, *Integral Equation Methods for Electromagnetic and Elastic Waves*. Morgan & Claypol Publishers, 2009.
- [14] J. Volakis and K. Sertel, *Integral Equation Methods for Electromagnetics*. IET, 2012.
- [15] D. W. Green, et al., "Chiral biomaterials: From molecular design to regenerative medicine," *Advanced Materials Interfaces*, 2016.
- [16] H. H. Pennes, "Analysis of tissue and arterial blood temperatures in the resting human forearm. 1948," *J. Appl. Physiol.*, vol. 85, no. 1, pp. 5-34, 1998.
- [17] C. Gabriel, "Compilation of the dielectric properties of body tissues at RF and microwave frequencies," *Brooks Air Force Base, TX, Report: AL/OE-TR-1996-0037, Tech. Rep.*, 1996.
- [18] H. Dodig, et al., "Stochastic sensitivity of the electromagnetic distributions inside a human eye modeled with a 3D hybrid BEM/FEM edge element method," *Eng. Anal. Bound. Elem.*, vol. 49, pp. 48-62, 2014.
- [19] K. R. Foster, et al., "Dielectric properties of brain tissue between 0.01 and 10 GHz," *Phys. Med. Biol.*, 1979.
- [20] D. Xiu, "Fast numerical methods for stochastic computations: A review," *Communications in Computational Physics*, vol. 5, no. 2, pp. 242-272, 2009.
- [21] D. Kroese, T. Taimre, and Z. Botev, *Handbook of Monte Carlo Methods*. John Wiley & Sons, New Jersey, USA: Wiley, 2011.
- [22] S. Lalléchère, et al., "An electromagnetic compatibility problem via unscented transform and stochastic collocation methods," *ACES Journal*, vol. 27, no. 2, pp. 94-101, 2012.
- [23] L. de Menezes, et al., "Efficient computation of stochastic electromagnetic problems using unscented transforms," *IET Sci. Meas. Technol.*, vol. 2, pp. 88-95, 2008.
- [24] A. Saltelli, et al., *Global Sensitivity Analysis - The Primer*, John Wiley & Sons Inc., Hoboken, USA: Wiley, 2008.
- [25] D. Thomas, O. Oke, and C. Smartt, "Statistical analysis in EMC using dimension reduction methods," in *Electromagnetic Compatibility (EMC), 2014 IEEE International Symposium on*, pp. 316-321, 2014.
- [26] T. Samaras, E. Kalampaliki, and J. Sahalos,

“Influence of thermophysiological parameters on the calculations of temperature rise in the head of mobile phone users,” *IEEE T. Electromagn. C.*, vol. 49, no. 4, pp. 936-939, 2007.

- [27] M. Cvetkovic, D. Poljak, and A. Hirata, “The electromagnetic-thermal dosimetry for the homogeneous human brain model,” *Eng. Anal. Bound. Elem.*, vol. 63, pp. 61-73, 2016.



Mario Cvetković received the B.S. degree in Electrical Engineering from the University of Split, Croatia in 2005, M.Phil degree from the Wessex Institute of Technology, University of Wales, UK, in 2009, and Ph.D. in 2013 from University of Split, Croatia, where he is currently working as a Postdoc. His research interests including numerical modeling including finite element and moment methods, computational bio-electromagnetics and heat transfer related phenomena.



Sébastien Lalléchère received the M.Sc. and Ph.D. degrees in Computational Modeling and Electronics/Electromagnetism from Polytech' Clermont and Blaise Pascal University, Clermont-Ferrand, France, in 2002 and 2006. He served as a Research Engineer in LASMEA, Clermont-Ferrand, France, in 2007 focusing on intensive computational methods for electromagnetics. He is currently an Associate Professor at Blaise Pascal University and Institut Pascal, Clermont-Ferrand, France. His research interests cover the fields of EMC including antennas and propagation, complex and reverberating electromagnetic environments, computational electromagnetics, stochastic modeling and sensitivity analysis in electrical engineering.



Khalil El Khamlichi Drissi received his M.Sc., and Ph.D. degrees in Electrical Engineering from Ecole Centrale de Lille and the University of Lille, in 1987 and 1990 respectively. He received the Habilitation in electronics, at the Doctoral School “Sciences Pour l’Ingénieur” of Blaise Pascal University, in 2001. Currently, he is Professor at the Department of Electrical Engineering where he was the Dean in the period from 2007 to 2011. He is also Senior Researcher at Institute Pascal Laboratory and his research interests include

EMC in Power Electronics and Power Systems, in particular numerical modeling, EMI reduction and converter control.



Pierre Bonnet received the Ph.D. degree in Electromagnetism from Blaise Pascal University, Clermont-Ferrand, France. From 1999 to 2008 he was an Assistant Professor within the Department of Physics and Institut Pascal at Blaise Pascal University. He is currently a Full Professor in this University and the head of the EMC group of Institut Pascal. His research interests are in the area of numerical electromagnetics with an emphasis on EMC/EMI problems, time reversal, source identification and stochastic approaches.



Dragan Poljak received his B.Sc. in 1990, his M.Sc. in 1994 and Ph.D. in Electrical Engineering in 1996 from the University of Split, Croatia. He is the Full Professor at Department of Electronics, FESB at the University of Split, and he is also Adjunct Professor at Wessex Institute of Technology. His research interests include frequency and time domain computational methods in electromagnetics, particularly in the numerical modelling of wire antenna structures, and numerical modelling applied to environmental aspects of electromagnetic fields. From 2011 to 2015 Poljak was the Vice-Dean for research at FESB. In 2011, Poljak became a Member of WIT Board of Directors while in June 2013, he became a Member of the board of the Croatian Science Foundation.